The Disulphide Group in Organic Compounds: Conformational Dependence of Core and Valence Sulphur Electronic Levels by *X*-Ray Photoelectron Spectroscopy

Joseph Riga and Jacques J. Verbist *
*Facultés Universitaires Notre-Dame de la Paix, Laboratoire de Spectroscopie Electronique,
Rue de Bruxelles, 61, B-5000 Namur, Belgium*

An *X*-ray photoelectron spectroscopic study is reported on symmetric acyclic aliphatic disulphides and cyclic or acyclic aromatic disulphides. Core-level binding energies and sulphur lone-pair peculiarities (energy splitting, binding energy, and peak intensity) provide detailed information on the conformation of the C–S–S–C entity (C–S and S–S bond lengths, CSS/SSC dihedral angle). These relations are then applied in cases where crystallographic data are not available (di-n-butyl disulphide, di-n-hexyl disulphide, and 2,2′-dinaphthyl disulphide).

The S–S bond appears as an important structural feature of many inorganic, organic and biological compounds and as such is known to play a major role in the functioning of some biological systems.[1] As the properties of the compound are related to conformation of the CSSC moiety, there is considerable interest in obtaining information about the disulphide framework geometry.

The flexibility of the sulphur–sulphur bond is remarkable: the bond lengths are found to be between 1.8 and 2.1 Å, the bond angles between 90 and 180°, and the CSS/SSC dihedral angles between 0 and 180°. Moreover, S–S stretching frequencies vary from 175 to 820 cm^{-1} and force constants from 1.4 to 6.3 mdyn Å^{-1}.[2]

In the field of organic disulphides, various empirical proposals have been offered to account for the variability of the S–S bond. Hordvik suggested that the bond lengths varies with the CSS/SSC torsion angle.[3] Noting the failure of this correlation among some disulphides, Shefter,[4] Kadooka *et al.*[5], Raghavan and Seff,[6] and Higashi *et al.*[7] proposed a correlation with another torsion angle, X–C–S–S, where X is C or N.

The relationship between the CSS/SSC dihedral angle (Θ) and bond lengths in H_2S_2 has been extensively studied by Saethre [8] in a CNDO/2 theoretical approach. In fact, in the field of theoretical chemistry, the molecular orbitals (MO) of disulphides have been the subject of numerous papers in order to interpret experimental results, to shed light on the conformational properties of the CSSC fragment, and to estimate the internal rotation barriers. Most commonly, the variations in MO eigenvalues and shapes are studied as a function of rotation around the S–S axis.[9–18]

From an experimental point of view, several works have shown that Raman spectroscopy is a useful technique for the study of S–S and C–S stretching behaviour, and a linear dependence of S–S stretching frequency on dihedral angle Θ has been found.[19–21] In another domain, a correlation has been reported between the energy of the lowest energy u.v. transition and the Θ angle.[9] From u.v. photoelectron spectroscopy (UPS), the energy splitting of the π sulphur lone pairs is also dependent on the Θ angle, and correlations have been reported [22–24] and used, *e.g.* in the case of sulphur-bridged *peri*-naphthalenes [25] and di-*tert*-adamantyl disulphide.[26]

The aim of this work is to demonstrate how an *X*-ray photoelectron spectroscopic (XPS) study of the C 1*s* and *S* 2*p* core levels and the sulphur π lone-pair molecular orbital can yield a detailed picture of the CSSC entity, including not only the dihedral angle value but also the C–S and S–S bond lengths.

In spite of lower resolution than UPS, the sulphur lone-pair peak presents clear characteristics (position, splitting, intensity) within the XPS valence band, which for the rest will be interpreted within the reasonable limits of confidence.

It should be noted that the present status (usually gas phase) UPS results do not permit the construction of a similar model of the CSSC moiety, but they provide, when available, useful complementary data.

Experimental

The work is focused on symmetric organic disulphides. The names and formulae of the studied molecules are listed in Table 1. They have been filed in three categories: (i) the acylic aliphatic disulphides, with the S–S bond bridging saturated carbon atoms (group I); (ii) the acyclic aromatic disulphides, with the S–S bond inserted between two sp^2 carbon atoms (group II); and (iii) the cyclic aromatic disulphides, characterized by a Θ angle smaller than 90° (group III).

The XPS spectra have been recorded on a Hewlett-Packard 5950 A spectrometer using monochromatized Al $K_{\alpha\ 1,2}$ radiation ($h\nu = 1\ 486.6$ eV). Powdered samples were pressed into pellets and deposited on a gold substrate. Except for TTN and TTT samples, an electron flood-gun was used during the analysis to compensate for the charging effect created by the ejection of the photoelectrons. In order to preserve the high vacuum required in the analysis chamber ($\simeq 1 \times 10^{-9}$ Torr), diphenyl disulphide and dibenzyl disulphide were cooled down to 265 K. The other samples were studied at the normal operating temperature ($\simeq 315$ K). In a solid-state XPS study, only the Fermi level of a conducting solid (gold in our case) can be taken as reference. The difference between the Fermi and the common vacuum levels is defined as the work function of the compound. In practice, the gold decoration technique consists in depositing a very thin film of gold on the sample surface; the strong Au 4*f* doublet, whose position with respect to gold Fermi level is known from a separate experiment, can be used as reference. However, owing to the lability of many organic samples, we have used an indirect calibration method that consists in mixing the sample with a known pre-calibrated compound having similar dielectric properties and distinct peaks. Two such calibrations were achieved independently: firstly, with cyclo-octasulphur, for which the binding energy, E_B of the S $2p_{\frac{3}{2}}$ core level is known to be 164.25 eV with respect to Au $4f_{\frac{7}{2}}$ at 84.0 eV; [27] secondly, with polyethylene, for which E_B C 1*s* = 284.5 eV,[27] using the same method. The results of the two experiments agreed to within 0.1 eV.

Owing to the high surface sensitivity of the XPS, the absence of oxygen has been thoroughly verified. Even after long accumulations, the surface was free from such contamin-

Table 1. Structural formulae of studied organic disulphides

Group I: acyclic aliphatic disulphides	
Dimethyl disulphide	$CH_3{-}S{-}S{-}CH_3$
Di-n-butyl disulphide	$CH_3(CH_2)_3S{-}S(CH_2)_3CH_3$
Di-n-hexyl disulphide	$CH_3(CH_2)_5S{-}S(CH_2)_5CH_3$
Dibenzyl disulphide	$C_6H_5{-}CH_2{-}S{-}S{-}CH_2{-}C_6H_5$
Dicinnamyl disulphide	$C_6H_5{-}CH{=}CH{-}CH_2{-}S{-}S{-}CH_2{-}CH{=}CH{-}C_6H_5$
Group II: acyclic aromatic disulphides	
Diphenyl disulphide	$C_6H_5{-}S{-}S{-}C_6H_5$
2,2′-Dinaphthyl disulphide	$C_{10}H_7{-}S{-}S{-}C_{10}H_7$
Group III: cyclic aromatic disulphides	
2,2′-Dithiobiphenyl	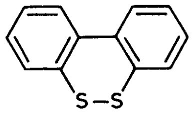
Tetrathionaphthalene (TTN)	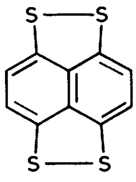
Tetrathiotetracene (TTT)	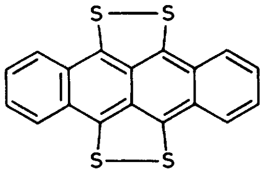

ation, as verified by the absence of the O 1*s* peak around 530 eV and of any O 2*s* features around 24 eV in the valence band spectra (see Figures 3, 7, 8, and 9).

Further details about the XPS technique can be found in recent books [28–30] and in a recent review paper.[31]

Structural Aspects

The structural characteristics of the molecules studied are reported in Table 2.[32–41] In acyclic compounds, the CSS/SSC dihedral angle is often found to be about 90° (except for dicinnamyl disulphide) and this conformation yields short S–S and long C–S bond lengths. This preferred geometry is easily explained by the fact that it minimizes the repulsive interactions between the sulphur π lone pairs (Figure 1). Some authors add that the shortness of the S–S bond is also partly due to π bonding, S_A $3p_z$–S_B $3d_{xy}$ or S_B $3p_y$–S_A $3d_{xy}$, which is most pronounced at $\theta = 90°$.[3,8]

Ab initio calculations have been performed on the simplest disulphide, namely H_2S_2, in the framework of the standard single determinantal molecular orbital theory. The atomic sets used in the computations were minimal: 1*s*-type orbital for hydrogen and 1*s*, 2*s*, $2p_x$, $2p_y$, $2p_z$, 3*s*, $3p_x$, $3p_y$, $3p_z$-type orbitals for sulphur. Each Slater-type orbital was least-squares fitted to a sum of three gaussian functions (STO-3G technique). The ' Gaussian 70 ' system has been used in its standard (75 orbitals) version.[42] The total energy of the molecule *versus* the dihedral angle is reported in Figure 2 and confirms the greatest stability for the $\Theta = 90°$ conformation. In the next section (b), we will compare the shape of this curve with that obtained by plotting the sulphur lone-pair splitting *versus* Θ (Figure 4). The *ab initio* results indicate here that a dihedral angle of 180° gives a more stable geometry than $\Theta = 0°$ by avoiding the steric hindrance between the hydrogens.

Table 2. Structural data of studied organic disulphides

Compound [a]	C–S (Å)	S–S (Å)	CSS/SSC angle (°)	Ref.
Dimethyl disulphide (5)	1.806	2.022	83.9	32
	1.816	2.029	85.3	33
Dibenzyl disulphide (6)	1.84	2.015	92.1	34
Dicinnamyl disulphide (7)	1.88	2.008	66.4	35
	1.858	2.020	74.3	36
Diphenyl disulphide (4)	1.80	2.03	96.2	37
	1.788	2.023		38
2,2′-Dithiobiphenyl (3)	1.757	2.050	68.7	39
Tetrathionaphthalene (2)	1.765	2.096	0	40
Tetrathiotetracene (1)	1.781	2.100	0	41

[a] The numbers refer to Figures 5 and 6.

If the S–S bond becomes part of a heterocycle, smaller values are found for Θ (Table 2). As a limit, a planar CSSC conformation is reached for TTN [40] and TTT.[41] This reduction of Θ increases the repulsive interactions between the π sulphur

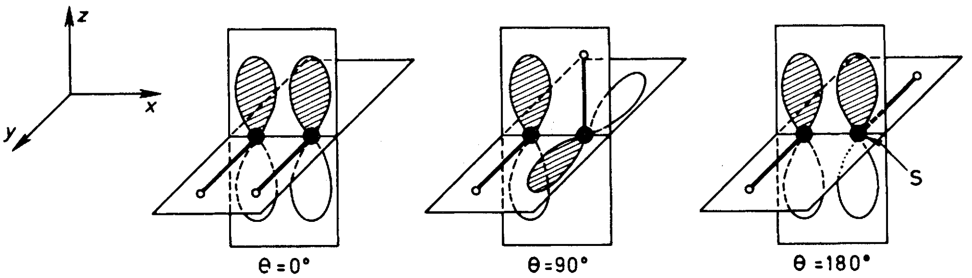

Figure 1. Sulphur lone pairs interaction *versus* dihedral angle

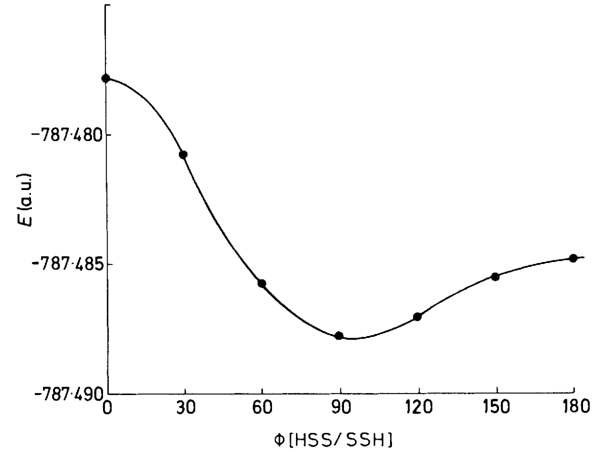

Figure 2. Total energy of H_2S_2 *versus* dihedral angle; H_2S_2-*ab initio* (STO-3G) calculations

lone pairs (Figure 1) and induces a lengthening of the S–S bond and a shortening of the C–S bond.

The following section describes how all these structural characteristics can be monitored in considerable detail by *X*-ray photoelectron spectroscopy.

Relation Between Valence Levels Data and Structure

(a) *Sulphur π Lone-pair Peak Intensity and C–S Bond Length.*—Figure 3 represents the XPS valence band spectra of four typical disulphides: group I (Table 1) is illustrated by dibenzyl disulphide, group II by diphenyl disulphide and group III by 2,2′-dithiobiphenyl ($\Theta = 68.7°$) [39] and TTN ($\Theta = 0°$).[40]

In the energy region between 25 and 9 eV are located the peaks corresponding to the MO that describe the C 2*s*–C 2*s*, C 2*s*–C 3*s*, and S 3*s*–S 3*s* chemical bonds. As the number of C–C bonds is, in each case, 5—7 times greater than the number of C–S or S–S bonds, this part of the spectra is dominated by the fingerprint of the corresponding acene (peaks E, F, G, H): benzene [43] for dibenzyl and diphenyl disulphides, biphenyl [44] for 2,2′-dithiobiphenyl and naphthalene [45] for TTN. The fact that the spectrum is less well resolved and the presence of some additional features are of course due to the presence of the C 2*s*–S 3*s* and S 3*s*–S 3*s* levels. A detailed analysis of this energy region is made in refs. 27 and 40. Below 9 eV, we find the C 2*p*–C 2*p*, C 2*p*–H 1*s*, and C 2*p*–S 3*p* MO and the sulphur lone-pair orbitals.

UPS results on some gaseous organic disulphides [21–25] and theoretical calculations on dimethyl disulphide and naphthalene 1,8-disulphide [46] reveal the sulphur lone-pair nature of the highest occupied molecular orbital (HOMO) (peak A, Figure 3), but the atomic population of the S 3*p* orbital in this level is related to the degree of localization of this lone pair on the chalcogen.

According to Gelius,[47] the photoelectronic cross-section of a molecular orbital *j*, I_j, results from a linear combination of *s*, *p*, *d*, . . . contributions for all the atoms of the molecule

$$I_j \propto \sum_{X\lambda} P_{X\lambda j}\ \sigma_{X\lambda}/\sigma_{X_0\lambda_0} \qquad (1)$$

[equation (1)]. In this equation $\sigma_{X\lambda}/\sigma_{X_0\lambda_0}$ is the relative cross section for the atom X with angular momentum λ ($\lambda = s, p, d, \ldots$) and $P_{X\lambda j}$ is the atomic population of the Xλ atomic orbital for the molecular orbital *j*.

Scofield's calculations [48] yield a relative scale of the atomic orbitals cross sections: σ C 2*p* = 10, σ S 3*p* = 52, σ H 1*s* $\simeq$ 0. These values clearly indicate that the XPS spectrum will favour MOs with large S 3*p* character. Therefore, the intensity of peak A (Figure 3) will be strongly affected, depending on whether the HOMO has or does not have a large S 3*p* character, in other words, whether the sulphur π lone pair is localized on the chalcogen or delocalized. We must underline that such information would be hindered in UPS by the strong dependence of the S 3*p* atomic orbital cross section on the photoelectron kinetic energy. In XPS, the photoelectron kinetic energy is relatively much less modified by the variations of the valence orbital binding energy.

In the case of dibenzyl disulphide, the high intensity of peak A (Figure 3) is due to a large S 3*p* contribution in the HOMO, *i.e.* to a strong localization of the π lone pairs on the two sulphur atoms. This observation is clearly related to the presence of the CH_2 group inserted between the chalcogen and the phenyl ring.

In diphenyl disulphide, the corresponding peak is less intense. According to equation (1) the HOMO contains some percentage of atomic orbitals with lower cross-section than S 3*p*. Spatially and energetically, only a π(S 3*p*–C 2*p*) mixture can occur. Indeed, the conformation of diphenyl disulphide ($\Theta = 96.2°$,[37] Table 2) sets each chalcogen lone pair nearly perpendicular to the benzene rings or parallel to the π C 2*p* cloud. Moreover, the energy value of the highest occupied π orbital of benzene ($E_B 1_{1g}$ = 3.9 eV [43]) is near the sulphur lone-pair binding energy. This π (S 3*p*–C 2*p*) interaction yields two MOs for each C–S bond: an antibonding mixture, π_-, at lower binding energy (peak A) and a bonding mixture, π_+, at higher binding energy (peak C). If the interaction is weak, the C 2*p* orbital contribution in π_- is small (*e.g.* in diphenyl disulphide). However, if the interaction is strong, (*e.g.* in TTN), the π_- MO has a large C 2*p* character, and peak A has a low intensity. On the other hand, the π_+ MO has a strong S 3*p* percentage and peak C is more intense in the XPS spectrum.

From Figure 3, it appears that the intensity of peak A strongly decreases from dibenzyl disulphide to TTN. This evolution is directly related to the C–S bond lengths: long in dibenzyl disulphide (single bond), shorter in diphenyl di-

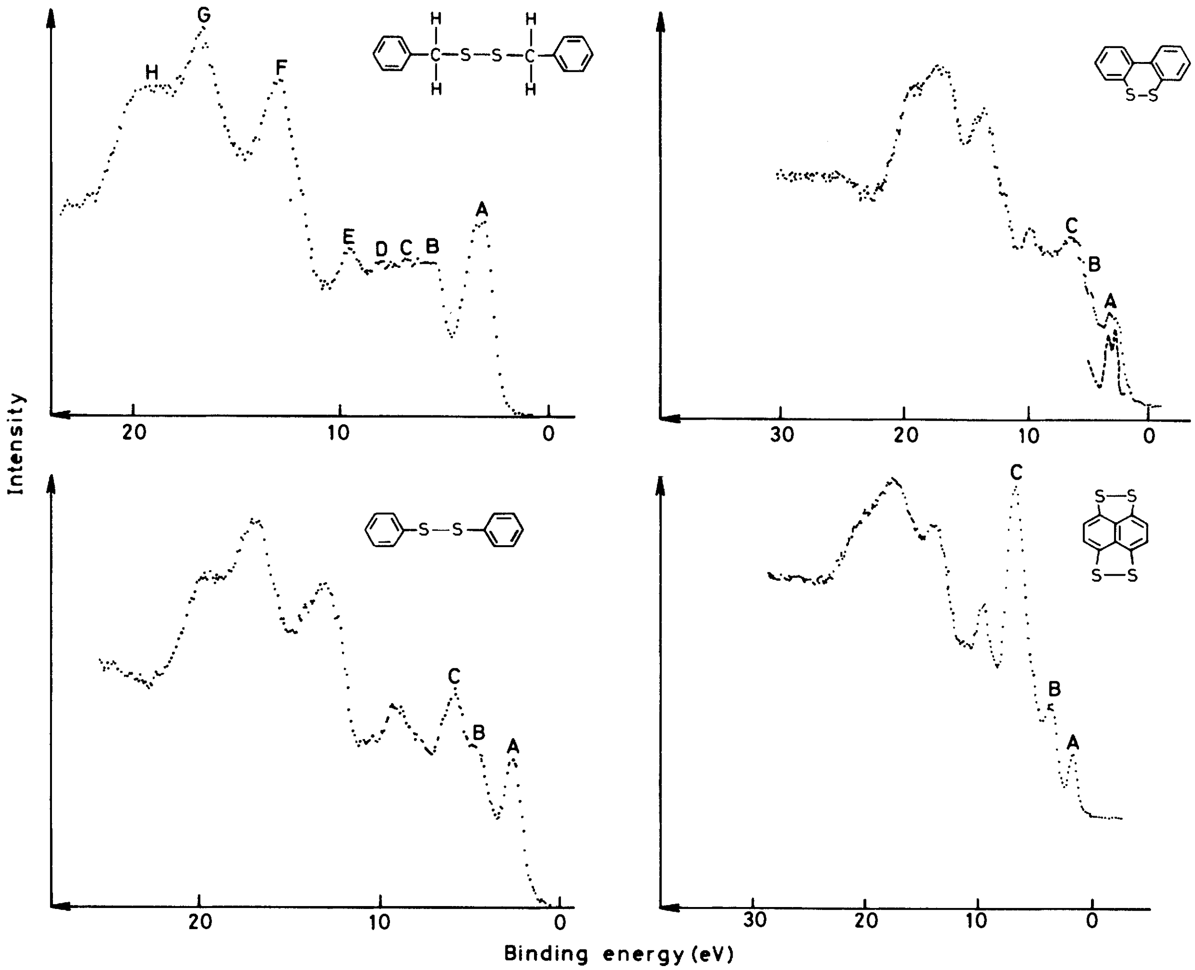

Figure 3. XPS valence band spectra of dibenzyl and diphenyl disulphides, of 2,2'-dithiobiphenyl, and of tetrathionaphthalene (TTN)

sulphide, and 2,2'-dithiobiphenyl, and very short in TTN (large double-bond character).

As a consequence the intensity of the HOMO in the XPS spectrum appears to be a powerful tool to assess the degree of the π interaction between the chalcogen and the carbon skeleton, and therefore to estimate the C–S double bond character.

(b) *Sulphur Lone-pair Energy Splitting and CSS/SSC Dihedral Angle.*—Some UPS measurements relating the S $3p$ lone-pair splitting to the value of the dihedral angle Θ have already been reported.[22–24] Let us briefly recall that following the Pauli principle, the electronic interaction between the two sulphur π lone pairs yields a bonding level, n_+, and an anti-bonding level, n_-. If Θ is near 90°, the splitting is around 0.2 eV [22–25] and cannot be observed in the XPS spectrum. If Θ decreases, the splitting is more pronounced. In 2,2'-dithiobiphenyl, peak A appears to have two components, n_- and n_+, separated by 0.7 eV (Figure 3). In TTT and TTN, the splitting is a maximum: more than 2.0 eV from theoretical prediction.[46] Therefore, the n_- and n_+ MOs are well separated. Peak A corresponds only to the n_- component, whereas the n_+ MO is now part of peak B. In the other spectra the main component of this peak B is a MO describing the σ(S $3p$–S $3p$) bond. Table 3 includes previous data published in the literature. Adding results, we are able to describe the $\Delta E(n_-/n_+)$ *versus* Θ relation [24] between 0 and 110° (Figure 4). An extrapolation of the curve to larger values of the dihedral angle is hindered by the lack of experimental data.

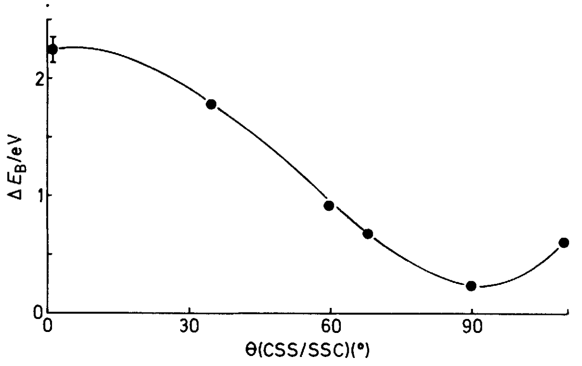

Figure 4. Sulphur lone-pair energy splitting *versus* dihedral angle

It is interesting to note that the form of this curve is similar to the theoretical curve representing total energy *versus* Θ in H_2S_2 (Figure 2). The repulsive interactions between the sulphur electron lone pairs appear therefore as a determining criterion in the stability of the conformation. However, we must keep in mind that in some cases the solid-state effects play a dominant role in the conformation and the resulting electronic structure of the molecule. Thus, the XPS valence

Table 3. Sulphur lone-pair energy splitting (ΔE) and CSS/SSC dihedral angle of selected disulphides

Compound	ΔE/eV	Ref.	Dihedral angle (°)	Ref.
CH_3SSCH_3	0.25	23	83.9	32
			85.3	33
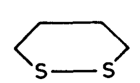	0.95	23	60	49
$(CH_3)_3CSSC(CH_3)_3$	0.65	23	110	14
	0.60	24		
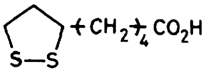	1.80	24	30	50
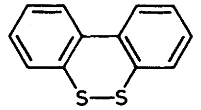	0.70	This work	68.7	39
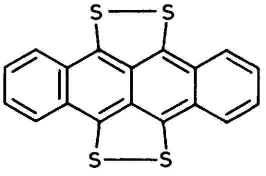	2.3	This work	0	41
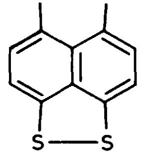	2.0	This work	0	40

Table 4. XPS data (values in eV)

Compound	E_B C 1*s* [a]	E_B S $2p_{\frac{3}{2}}$	E_B S 3*p* [b]
Dimethyl disulphide	284.5	164.0	3.6
Di-n-butyl disulphide	284.5	163.8	3.4
Di-n-hexyl disulphide	284.5	163.6	3.2
Dibenzyl disulphide	184.5	163.9	3.6
Dicinnamyl disulphide	284.5	163.85	3.55
Diphenyl disulphide	284.5	164.3	2.9
2,2′-Dinaphthyl disulphide	284.5	164.2	2.75
2,2′-Dithiobiphenyl	284.5	164.3	3.4—2.7
Tetrathionaphthalene (TTN)	283.8	164.4	3.5—1.5
Tetrathiotetracene (TTT)	283.9	164.35	3.2—0.9
Cyclo-octasulphur (S_8)		164.25	3.6

[a] Centroid of the C 1*s* signal, except in TTN and TTT where the values correspond to the four C_α components. [b] Centroid of the peak except if it is possible to distinguish the n_+ and n_- components.

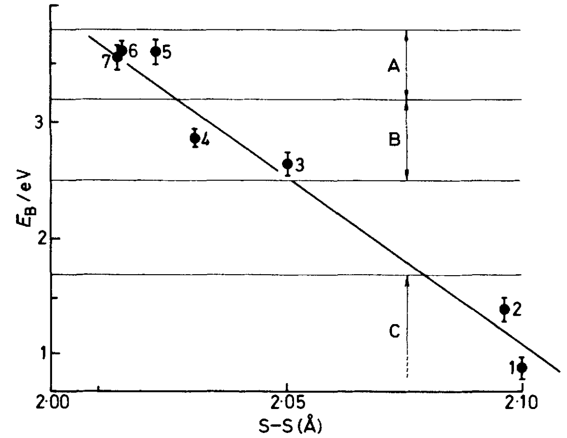

Figure 5. Sulphur lone-pair binding energy *versus* S–S bond length (the numbers refer to Table 2). Region A, aliphatic disulphides; B, non-planar aromatic disulphides; C, planar aromatic disulphides

band spectra of dicinnamyl and dibenzyl disulphides appear very similar whereas Lee and Bryant [35] reported an unusually small CSS/SSC dihedral angle (Θ = 66.4°) for the first of these linear compounds. Its other peculiarities include a short S–S bond (2.008 Å) and a long C–S bond (1.88 Å) compared with dibenzyl disulphide. Another structure determination was made by Donohue and Chesick [36] in 1975. Their results, Θ = 74.3° and C–S and S–S bond lengths, more similar to the dibenzyl derivative, (Table 2), appear in better agreement with XPS information.

However, by using the ΔE *versus* Θ relation, we should observe a sulphur lone-pair energy splitting of 0.5 eV if Θ = 74.3°, and 0.75 eV if Θ = 66.4°. In fact, on the XPS spectrum, the S 3*p* peak appears single, with a full width at half-maximum similar to dibenzyl disulphide, for which Θ = 92.1°. This lack of splitting or broadening can perhaps be explained by the peculiar conformation of dicinnamyl disulphide. Short H $\cdots$ S distances indeed suggest intramolecular hydrogen bonds, which allow a delocalization of the charge density from the lone pairs, thus reducing the electronic repulsion.

(c) *Sulphur Lone-pair Binding Energy and S–S Bond Length.*—A complete picture of the CSSC fragment is obtained by examining the relation between the S–S bond length and the sulphur π lone-pair binding energy, which is a measure of its degree of delocalization.

In the aliphatic systems (group I in Table 1), the lone-pair orbital is strictly localized on the sulphur atom [see section (a)] and its binding energy is large (Table 4). In an aromatic system, such as diphenyl disulphide, electron delocalization into the benzenic group is possible and the HOMO (n_- S 3*p*–C 2*p*) shifts to the Fermi level. Simultaneously, the S–S bond weakens. The most important delocalization is observed in TTT: E_B HOMO is only equal to 0.8 eV, and the compound exhibits semiconducting properties of great interest because of its electron-donor ability.[51,52]

This relation is depicted in Figure 5. Again we find three groups: around 3.5 eV the aliphatic disulphides; next the acyclic and cyclic non-planar aromatic disulphides (3.0 $\geqslant E_B$ HOMO $\geqslant$ 2.5 eV); and below 1.5 eV, the planar aromatic compounds.

Core Level Analysis

The C 1*s* and S $2p_{\frac{3}{2}}$ core-level positions yield a relation between the difference in the S and C_α atomic charges (*q*) and the S–S bond length, d(S–S). This difference in atomic charges is measured by the quantity E_B C 1*s* − E_B S $2p_{\frac{3}{2}}$: a more positive charge on carbon increases E_B C 1*s* and a more negative charge on the sulphur atom decreases E_B S $2p_{\frac{3}{2}}$ (Table 4). We again find three energy regions in Figure 6. (i) The aliphatic disulphides; with ΔE_B between 121.0 and 120.5 eV, for S–S bond lengths going from 2.010 to 2.025 Å. These compounds are characterized by a small negative charge on the sulphur atoms. (ii) The acyclic and cyclic non-planar aromatic disulphides with ΔE_B between 120.1 and 120.4 eV and *d* S–S = 2.030—2.050 Å. In this group, q_S is near zero. (iii) The planar aromatic disulphides: ΔE_B = 119.6 ± 0.3 eV and *d* S–S = 2.090—2.100 Å. These molecules are characterized by a small positive charge on the sulphur and a negative charge on

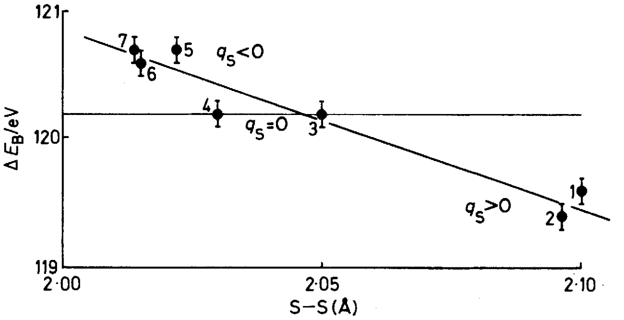

Figure 6. Core level binding energy difference (E_B C 1*s* − E_B S $2p_{\frac{3}{2}}$) *versus* S–S bond length (the numbers refer to Table 2); q_S is the sulphur atomic charge

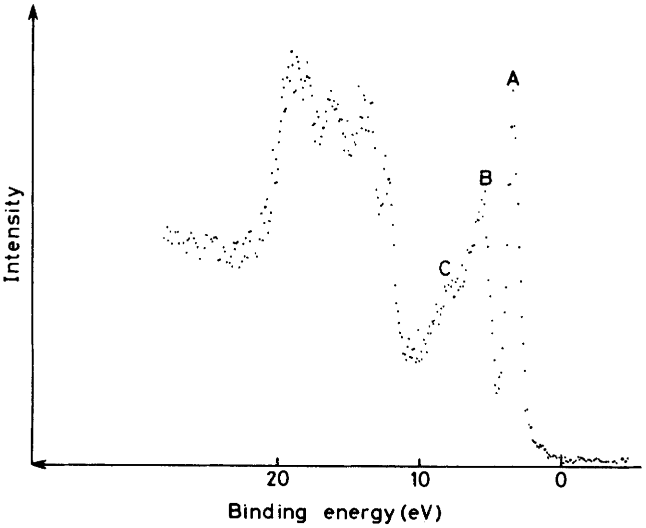

Figure 7. XPS valence band spectrum of di-n-butyl disulphide

the adjacent carbon atoms.[40] Only in TTT and TTN is it possible to distinguish the C_α from the other carbon atoms in the C 1*s* signal. Therefore we estimate E_B C_α 1*s* in the two first categories as the C 1*s* peak centroid (284.5 eV). In these compounds, a weak shake-up satellite associated with the high π-electron density in the C–S bond region has been reported in a previous paper.[40]

Application of the Correlations

In order to illustrate the applications of the described relations, we have studied three organic disulphides for which the crystallographic data are not available: two acyclic aliphatic disulphides, di-n-butyl disulphide and di-n-hexyl disulphide; and one acyclic aromatic disulphide, 2,2′-dinaphthyl disulphide.

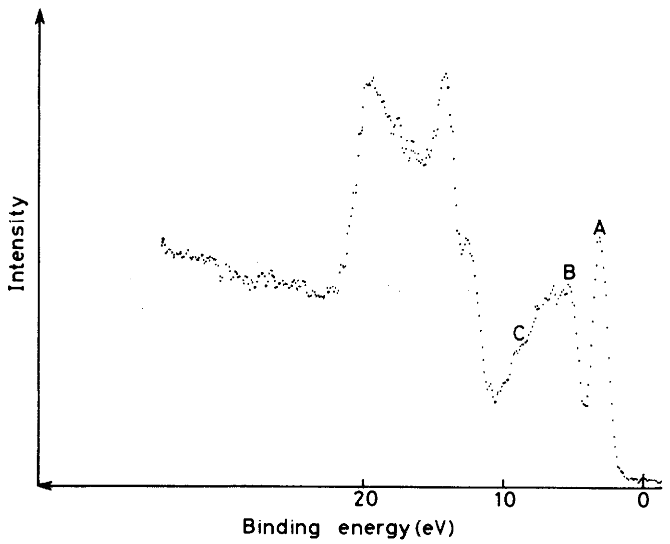

Figure 8. XPS valence band spectrum of di-n-hexyl disulphide

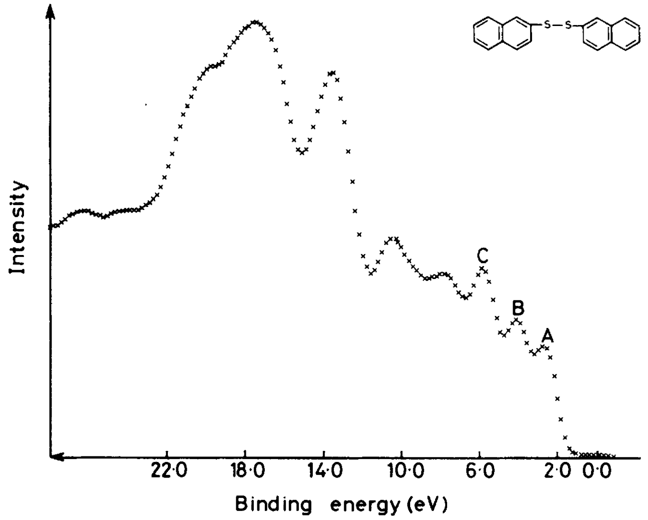

Figure 9. XPS valence band spectrum of 2,2′-dinaphthyl disulphide

Their XPS valence band spectra are shown in Figures 7—9 and the core and valence level binding energies are given in Table 4. In the first two cases, the sulphur lone-pair intensity (labelled A in Figures 7 and 8) clearly shows that the corresponding MO is strictly localized on the chalcogen. Therefore, there is no double character in the C–S bond. As no splitting or broadening is observed on peak A, the CSS/SSC dihedral angle must be *ca.* 90°. The two correlations that involve the S–S bond length also indicate that the CSSC conformation in these two compounds is very similar to that which is observed in dimethyl disulphide. Therefore, we predict the following structural data: $85° < \Theta < 90°$; $1.81 < d\text{C–S} < 1.82$ Å, and $2.02 < d\ \text{S–S} < 2.03$ Å. We must note here that the shift of the S 2*p* and S 3*p* levels to the low binding energy (Table 4) reflects the increasing inductive effect of the aliphatic chain, which induces a more negative charge on the chalcogens.

From our XPS results on 2,2′-dinaphthyl disulphide (Figure 9 and Table 4), the CSSC fragment adopts a similar geometry to that of diphenyl disulphide. Unlike the aliphatic compounds, the S 3*p* level shift to the Fermi level arises from the π S 3*p* − C 2*p* interaction. This is clearly confirmed by the fact that (i) the E_B S 2*p* core level is constant; (ii) the S 3*p* lone pair peak intensity (peak A in Figure 9) decreases.

The information on the CSSC fragment can also explain specific reactions. For example, new reactions of some disulphides involving insertion of tetrafluoroethylene at the C–S bond have been found.[53] The fact that diphenyl disulphide but not dibenzyl disulphide undergoes this reaction is explained by the double character of the C–S bond in the case of the aromatic derivative, as clearly shown by *X*-ray photoelectron spectroscopy.

Conclusions

X-Ray photoelectron spectroscopy has been applied to characterize the conformation of the CSSC moiety in various unsubstituted symmetric organic disulphides. Core and valence-level characteristics of sulphur (intensity and binding energy) have yielded detailed information on the geometry of the molecule. Relations have been found between the binding-energy difference of the C $1s$ and S $2p$ core levels and the S–S bond length. The sulphur lone-pair signal was found to be particularly informative: its energy splitting is related to the CSS/SSC dihedral angle, its binding energy sheds light on the S–S bond, and the intensity of the photoemission is directly connected to the C–S double-bond character.

The potentialities of the XPS technique have been used to explain particular chemical reactivity and to predict conformation of some disulphides for which the *X*-ray crystallographic data are not available. However, caution must be used because of other factors that can affect the XPS data. For instance, in the case of dicinnamyl, the importance of the intramolecular hydrogen bond has been underlined. We have also shown that, for example, an S $3p$ lone-pair chemical shift can reflect differences in either the photoemission intramolecular relaxation, the atomic charge on the chalcogen, or the π interaction. Therefore, each piece of information obtained concerning an electronic level must necessarily be confirmed by other features in the XPS spectrum.

Acknowledgements

The authors are very grateful to Professors I. Bernal (University of Houston, Texas) and F. Wudl (University of California at Santa Barbara) for helpful ideas and for supplying TTT and TTN samples, to Dr. O. Dideberg (University of Liège), Professor I. T. Millar (University of Keele), and Dr. G. W. Smith (BP Research Centre, Sunbury on Thames) for making, respectively, TTT, 2,2′-dithiobiphenyl, and dicinnamyl disulphide samples available. They wish to thank their colleagues of the Applied Theoretical Chemistry Laboratory, Professors J. M. André and J. Delhalk, Drs. D. Vercauteren and C. Lamotte, for helpful discussions and for making their programs available. They also thank Mr. Ph. Henrot for keeping the Hewlett-Packard spectrometer in perfect condition.

References

1 A. White, P. Handler, and E. L. Smith in 'Principles of Biochemistry,' McGraw-Hill, New York, 1964, p. 891, 3rd edn.
2 R. Steudel, *Angew. Chem., Int. Ed. Engl.*, 1975, **14**, 655, and references therein.
3 A. Hordvik, *Acta Chem. Scand.*, 1966, **20**, 1885.
4 E. Shefter, *J. Chem. Soc. B*, 1970, 903.
5 M. M. Kadooka, L. G. Warner, and K. Seff, *J. Am. Chem. Soc.*, 1976, **98**, 7839.
6 N. V. Raghavan and K. Seff, *Acta Crystallogr.*, 1977, **B33**, 386.
7 L. S. Higashi, M. Lundeen, and K. Seff, *J. Am. Chem. Soc.*, 1978, **100**, 8101.
8 L. J. Saethre, *Acta Chem. Scand., Ser. A*, 1975, **29**, 538.
9 D. B. Boyd, *J. Am. Chem. Soc.*, 1972, **94**, 8799.
10 D. B. Boyd, *Theor. Chim. Acta*, 1973, **30**, 137.
11 D. B. Boyd, *J. Phys. Chem.*, 1974, **78**, 1554.
12 A. Veillard and J. Demuynck, *Chem. Phys. Lett.*, 1970, **4**, 476.
13 H. Yamabe, H. Kato, and T. Yonezawa, *Bull. Chem. Soc. Jpn.*, 1971, **44**, 604.
14 J. P. Snyder and L. Carlsen, *J. Am. Chem. Soc.*, 1977, 99, 2931.
15 M. E. Schwart, *J. Chem. Phys.*, 1969, **51**, 4182.
16 H. E. Van Wart and H. A. Scheraga, *Proc. Natl. Acad. Sci. USA*, 1977, **74**, 13.
17 H. E. Van Wart, L. L. Shipman, and H. A. Scheraga, *J. Phys. Chem.*, 1975, 79, 1428.
18 F. S. Jørgensen and J. C. Snyder, *Tetrahedron*, 1979, **35**, 1399.
19 H. E. Van Wart and H. A. Scheraga, *J. Phys. Chem.*, 1976, **80**, 1812.
20 H. E. Van Wart, A. Lewis, H. A. Scheraga, and F. D. Saeva, *Proc. Natl. Acad. Sci. USA*, 1973, **70**, 2619.
21 H. E. Van Wart, L. L. Shipman, and H. A. Scheraga, *J. Phys. Chem.*, 1974, **78**, 1848.
22 H. Bock and G. Wagner, *Angew. Chem.*, 1972, **84**, 119.
23 G. Wagner and H. Bock, *Chem. Ber.*, 1974, **107**, 68.
24 M. F. Guimon, C. Guimon, and G. Pfister-Guillouzo, *Tetrahedron Lett.*, 1975, 441.
25 H. G. Guttenberger, H. J. Bestmann, F. L. Dickert, F. S. Jørgensen, and J. P. Snyder, *J. Am. Chem. Soc.*, 1981, **103**, 159.
26 G. Rindorf, F. S. Jørgensen, and J. P. Snyder, *J. Org. Chem.*, 1980, **45**, 5343.
27 J. Riga, Ph.D. Thesis, University of Namur, 1978, available from University Microfilms, Publ. No. 7970007.
28 T. Carlson, 'Photoelectron and Auger Spectroscopy,' Plenum Press, New York, 1975.
29 'Electron Spectroscopy, Theory, Techniques, and Applications,' ed. C. Brundle and A. Baker, Academic Press, 1977, vols. 1, 2, and 3.
30 'Photoemission in Solids, I and II,' ed. M. Cardona and L. Ley, Springer Verlag, Berlin 1978—1979.
31 Tran Minh Duc, Le Vide—les couches minces, 1981, **36**, 307.
32 B. Beagley and K. T. McAloon, *Trans. Faraday Soc.*, 1971, **67**, 3216.
33 J. D. Lee and M. W. R. Bryant, *Acta Crystallogr.*, 1969, **B25**, 2497.
34 A. Yokozeki and S. H. Bauer, *J. Phys. Chem.*, 1976, **80**, 618.
35 J. D. Lee and M. W. R. Bryant, *Acta Crystallogr.*, 1971, **B27**, 2325.
36 J. Donohue and J. P. Chesick, *Acta Crystallogr.*, 1975, **B31**, 986.
37 J. D. Lee and M. W. R. Bryant, *Acta Crystallogr.*, 1969, **B25**, 2094.
38 M. Sacerdotti, G. Gilli, and P. Domiano, *Acta Crystallogr.*, 1975, **B31**, 327.
39 I. Bernal and J. Ricci, personal communication.
40 J. Riga, J. J. Verbist, F. Wudl, and A. Kruger, *J. Chem. Phys.*, 1978, **69**, 3221.
41 O. Dideberg and J. Toussaint, *Acta Crystallogr.*, 1974, **B30**, 2481.
42 W. J. Hehre, W. A. Lathan, R. Ditchfield, M. D. Newton, and J. A. Pople, Quantum Chemistry Program Exchange, Indiana University, QCPE No. 236, 1973.
43 J. Riga, J. J. Pireaux, and J. Verbist, *Mol. Phys.*, 1977, **34**, 131.
44 J. Riga, J. J. Pireaux, J. P. Boutique, R. Caudano, J. J. Verbist, and Y. Gobillon, *Synth. Metals*, 1981, **4**, 99.
45 J. Riga, J. J. Pireaux, R. Caudano, and J. Verbist, *Phys. Scr.*, 1977, **16**, 346.
46 J. Riga, J. J. Verbist, C. Lamotte, and J. M. André, *Bull. Soc. Chim. Belg.*, 1978, **87**, 163.
47 U. Gelius, in 'Electron Spectroscopy,' ed. D. A. Shirley, North Holland, Amsterdam, 1972, p. 311.
48 J. H. Scofield, *J. Electron Spectrosc.*, 1976, **8**, 129.
49 O. Foss, K. Johnson, and T. Reistad, *Acta Chem. Scand.*, 1964, **18**, 2345.
50 L. A. Neubert and M. Carmack, *Tetrahedron Lett.*, 1974, 3542.
51 E. A. Perez-Albuerne, H. Johnson, Jr., and D. J. Trevoy, *J. Chem. Phys.*, 1971, **55**, 1547.
52 M. L. Khidekel and E. I. Zhilyaeva, *Synth. Metals*, 1981, **4**, 1, and references therein.
53 K. V. Dvornikova, A. M. Maksimov, V. E. Platonov, and G. G. Yakobson, IXth International Symposium on Organic Sulphur Chemistry, Riga (LSSR), 1980, Abstract A132.

Received 4th January 1983; Paper 3/003